Quaternary Science Reviews 30 (2011) 921–933

Contents lists available at ScienceDirect

Quaternary Science Reviews

journal homepage: www.elsevier.com/locate/quascirev

Compound-specific D/H ratios of the marine lakes of Palau as proxies for West Pacific Warm Pool hydrologic variability

R.H. Smittenberg [a,d,*], C. Saenger [b], M.N. Dawson [c], J.P. Sachs [d]

[a] ETH Zürich, Geological Institute, Sonneggstrasse 5, Room NO G47, 8092 Zürich, Switzerland
[b] Yale University, Department of Geology and Geophysics, New Haven, CT 06520, USA
[c] School of Natural Sciences, University of California, Merced, 5200 North Lake Road, Merced, CA 95343, USA
[d] University of Washington, School of Oceanography, Box 355351, Seattle, WA 98195, USA

ARTICLE INFO

Article history:
Received 29 September 2010
Received in revised form
17 January 2011
Accepted 19 January 2011
Available online 11 February 2011

Keywords:
West Pacific Warm Pool
Biomarkers
Hydrogen isotopes
Paleoclimate
Hydroclimate
Marine lakes
Palau

ABSTRACT

We tested the use of hydrogen isotopic ratios (δD) of lipids in marine lake sediments from the Micronesian Republic of Palau against the instrumental record of the last century to assess their capacity to record past hydrological changes of the Western Pacific Warm Pool. δD values of the algal lipid biomarker dinosterol (δD_{Dino}) and the more generic palmitic acid (δD_{PA}) were found to be sensitive indicators of the intensity of regional precipitation, as recorded by the Southern Oscillation Index (SOI). The observed sensitivity is caused by the combined effect of: 1) The amount effect in tropical precipitation; 2) Dilution of the isotopically heavy saline surface waters with light precipitation; 3) A salinity effect on the biosynthetic D/H fractionation between lipid and lake water. Both lake water δD (δD_{Lake}) and δD_{Dino} could be expressed as a quadratic function of either precipitation or lake water salinity. δD_{Dino} values were used to reconstruct past hydrological changes of the region. Long-term variations in the strength and sign of the El Niño - Southern Oscillation (ENSO) since the Little Ice Age (LIA, ~1450–1850 A.D.) and during the early Holocene (~7–9 kyr BP) appeared to dominate decadal variability, and indicate very dry conditions during the LIA. Early Holocene δD_{Dino} values were on average ~10‰ higher than those of recent centuries, which we interpret as a result of millennial scale hydrologic and water mass changes on a global level. The similar ~35‰ range of δD changes during the early Holocene and last several centuries imply a similar range of decadal-centennial hydrologic variability during those two climate regimes. Our results indicate that a correlation exists between solar irradiance levels and tropical Pacific climate.

1. Introduction

Recent research has improved understanding of the physical features and dynamics of tropical Pacific climate, yet many aspects are still only partly understood (Collins et al., 2010). Insights from coupled global circulation models (CGCMs) tested against global observational records during the satellite age contrast with the dearth of reliable observations of tropical climate, which rarely extend back more than a century and are spatially scattered, especially in oceanic regions. Proxy-based paleoclimate reconstructions thus provide invaluable information describing natural climate variability and dynamics prior to observational records, may help assess sources of model uncertainty, and allow important supplemental tests of model sensitivity to boundary conditions outside the range of observational records (Brown et al., 2008). Such reconstructions are scarce in the tropical Pacific, and there is an ongoing need to increase the number and type of paleoclimate reconstructions in the region.

The Western Pacific Warm Pool (WPWP) is a key component of tropical Pacific and global climate variability. Deep convection in this body of warm (>28 °C) surface water drives large fluxes of sensible and latent heat and moisture to the global atmosphere. The hydrological cycle is one of the most sensitive indicators of changes in the WPWP atmosphere-ocean system. Small variations in the size, position and temperature of the WPWP can have a large effect on tropical hydrology and therefore global climate (Trenberth et al., 1998; Cane, 1998; Pierrehumbert, 2000; Wang and Mehta, 2008). This, in turn, can affect oceanic and terrestrial ecosystems, as well as primary productivity (Behrenfeld et al., 2006; Woodward et al., 2008). In addition to local WPWP-forcing, tropical hydrology can be influenced remotely by high latitude cooling (Chiang and Bitz,

* Corresponding author. Future address: Department of Geological Sciences, Stockholm University, SE-106 91, Stockholm, Sweden. Tel.: +41 44 632 8474.
E-mail address: smittenberg@erdw.ethz.ch (R.H. Smittenberg).

0277-3791/$ – see front matter © 2011 Elsevier Ltd. All rights reserved.
doi:10.1016/j.quascirev.2011.01.012

2005; Broccoli et al., 2006), natural variations in solar activity (Bard and Frank, 2006) and anthropogenic climate change (Trenberth and Hoar, 1997; Collins et al., 2010). Finally, the WPWP is a driving factor in the El Niño-Southern Oscillation (ENSO), which interacts with the annual movement and strength of the Intertropical Convergence Zone (ITCZ) (e.g. Gagan et al., 2004).

Most reconstructions of tropical Pacific hydrology come from sites on or near continents (Wang et al., 2005; Partin et al., 2007; Yancheva et al., 2007; Griffiths et al., 2009; Tierney et al., 2009). At those sites ocean-driven climatic changes are mixed with continental effects such as orography or the vastly different moisture contents and heat capacity of land compared to the ocean. Reconstructions of the oceanic hydroclimate must therefore be sought farther from large landmasses. Although valuable paleohydrologic reconstructions have been generated from marine settings (e.g. Stott et al., 2004; Oppo et al., 2009; Abram et al., 2009; Newton et al., 2006), they are based primarily on the oxygen isotopic ratio of biogenic carbonate ($\delta^{18}O_{CaCO3}$). This reflects the $\delta^{18}O$ value of seawater, which is influenced by evaporation and precipitation processes – the same processes that influence salinity. As a result, $\delta^{18}O_{CaCO3}$ also typically co-varies with sea surface salinity (SSS). However, $\delta^{18}O_{CaCO3}$ can also be strongly influenced by sea surface temperature (SST). In many cases Mg/Ca or Sr/Ca thermometers have been used to correct for the temperature influence on $\delta^{18}O_{CaCO3}$, but the reliability of these ratios as pure SST proxies is under debate (e.g. Saenger et al., 2008; Dissard et al., 2010). Furthermore, many existing reconstructions from open ocean sites may not capture hydrologic variations well due to surface mixing or dampening by the large ocean reservoir. For instance, in the WPWP the ideal situation for the use of $\delta^{18}O_{CaCO3}$ exists in that the SST remains consistently warm and equable, while SSS can change by up to two psu in association with hydrological changes related to ENSO. Still, this only translates only to changes in coral $\delta^{18}O$ of *ca* 0.3‰ (Wu and Grottoli, 2010), i.e. just above the standard error of measurement (±0.15).

Here, we investigate the hydrogen isotopic ratio (δD) of lipids preserved in marine lake sediments from the WPWP island group of Palau as a paleohydrologic proxy. The islands are relatively small and low and lie in the maritime province of the WPWP, so that rainfall characteristics closely represent those of the ocean. A modern correlation between lipid δD and tropical hydrology is used as the basis for paleohydrologic reconstructions from the Little Ice Age (LIA, ~1450–1850 A.D.) and early Holocene (~7–9 kyr BP). LIA results, initially presented by Sachs et al. (2009), are explored in greater detail while early Holocene results are presented for the first time.

2. Study area

Palau (7–8°N, 134.5°E) (Fig. 1) is located within the WPWP and experiences significant hydrological variations that are broadly characteristic of the region. Modern variability is caused by a number of complex and interconnected ocean-atmosphere processes (Wang and Mehta, 2008). Warm SSTs and deep convection in the ascending limb of the meridional Hadley circulation are balanced by low-level convergence that creates a filament of intense ITCZ precipitation (Fig. 2a). Annual average precipitation in the region exceeds 3700 mm (Fig. 2a) and exhibits a seasonality caused by latitudinal migrations of the ITCZ. Precipitation is lowest from November–April and highest in June and July (Legates and Willmott, 1990; Spencer, 1993; Xie and Arkin, 1997; Figs. 2c, d and 3a). In addition to being a key factor in the meridional Hadley circulation, the WPWP's deep convection is part of the longitudinal Walker circulation, which is a primary component of ENSO. A good representation of ENSO in the West Pacific is the Southern

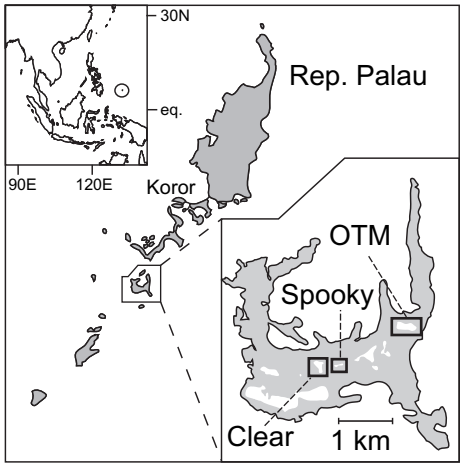

Fig. 1. Map of Palau and the investigated lakes: Ongeim'l Tketau (OTM; 7° 9.66′ N 134° 22.53′ E), Spooky lake (Spooky; 7° 9.14′ N 134° 21.76′ E) and Clear lake on the island of Mecherchar.

Oscillation Index (SOI), defined as the normalized pressure difference between Darwin, Australia and Tahiti. During an El Niño event, the Walker circulation shifts eastward, leading to large interannual precipitation anomalies (Figs. 2b and 3b). Annual precipitation in Palau during the El Niño years of 1983 and 1997 averaged 6.55 and 6.60 mm day^{-1}, respectively, compared to a climatological (1979–2000; Xie and Arkin, 1997) average of 8.85 ± 1.58 mm day^{-1}. The opposite is generally true of La Niña years, such as 1999 and 2000, during which a westward shift of the Walker circulation contributed to high annual average precipitation of 11.81 and 11.91 mm day^{-1}, respectively.

Recent precipitation δD values (δD_{Precip}) from Palau (Kurita and Ichiyanagi, 2008), and 1968–1976 values from nearby Yap atoll (9.46°N, 138.04°E) (IAEA, 2006) generally follow precipitation amounts (Fig. 3c, d). The average annual cycle for Palau shows enriched values near −5‰ in dry winter months and depleted values near −50‰ during the wet summer (Bowen, 2008; www.waterisotopes.org) (Fig. 3a). In the tropics, water isotopic variability has been strongly correlated with the amount of precipitation without a significant temperature influence (Araguás-Araguás et al., 1998).

The 'rock islands' of the Palau archipelago contain a cluster of ~70 marine lakes, which formed when the topographically complex karst landscape of uplifted Miocene reef was progressively flooded by rising sea level after the last glacial maximum (Hamner and Hamner, 1998 and references therein). The sediment cores analyzed in this study were collected from two such lakes, lying 1.5 km apart: Ongeim l'Tketau (OTM, also known as Jellyfish lake) and Spooky lake (Hamner and Hamner, 1998) (Fig. 1). The ~25 m deep OTM has a surface area of ~0.05 km^2, while Spooky Lake measures ~0.0125 km^2 and is ~13 m deep. Water profile data were also collected for the upper 10 m of a third, similar, lake called Clear lake, that has a maximum depth of 80 m.

High precipitation rates and limited lake water – seawater exchange through the island karst leads to strong density stratification and permanently anoxic bottom waters (Hamner and Hamner, 1998). The lakes fill and empty at the surface by gentle percolation through fissures and channels in the island karst and through dense thickets of lakeside mangrove roots. Exchange with outside lagoon water is never sufficient to remove the brackish surface layer that stabilizes and stratifies the water columns. The tidal range of lake OTM is around half that of the outside lagoon, and has a 2 h delay, while the range of Spooky and Clear lake is

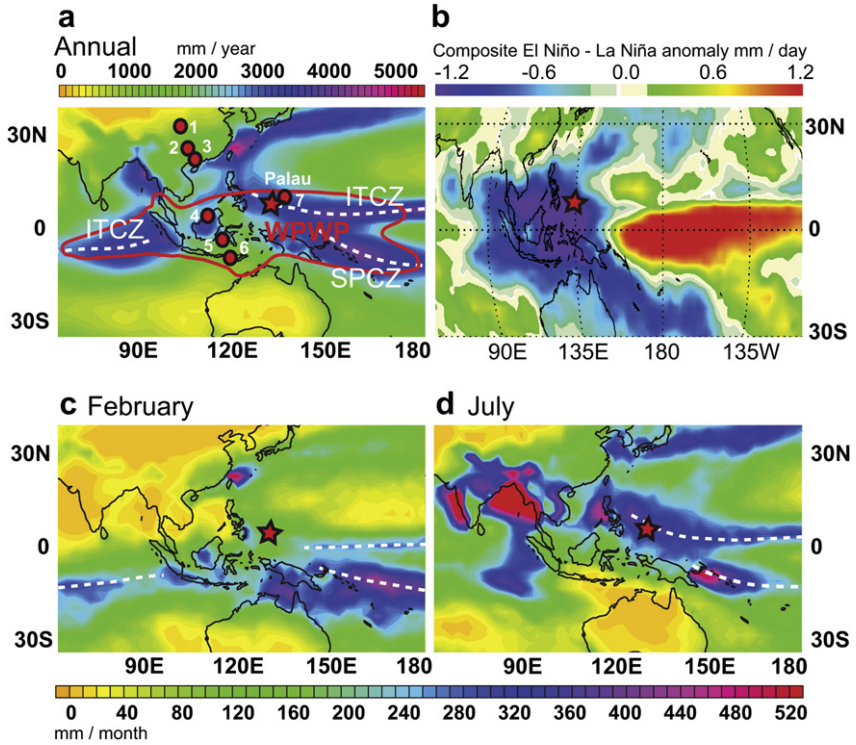

Fig. 2. Precipitation patterns of the West Pacific Warm Pool (WPWP) and the surrounding region. (a) Mean annual precipitation (1979–1992). Indicated are the approximate extent of the (WPWP) (after Yan et al., 1992), the Intertropical Convergence Zone (ITCZ) and the South Pacific Convergence Zone (SPCZ). b) Composite El Niño minus La Niña precipitation anomalies for 1979–1999 (Adler, 2003). c) Boreal winter (February) and d) summer (July) precipitation patterns. Data for a, c and d are from Legates and Willmott (1990) and Spencer (1993) available at http://jisao.washington.edu/legates_msu. Circles on the maps indicate locations of climate records discussed in the text: 1. Dongge cave; 2. Wanxiang cave; 3, Huguang Maar; 4. Borneo; 5. Makassar strait; 6. Liang Luar; 7. Yap. Palau is marked by the star.

around one quarter with a 3 h delay (Hamner and Hamner, 1998). The water that enters lake OTM from the lagoon moves rapidly into surface-level channels but then enters into narrow channels between mangrove roots and the surrounding rock walls so that the force entry has dispersed by the time flood waters reach the lake proper. Clear lake and Spooky lake do not have clear channels entering the lakes, and are also surrounded by thickets of mangroves. The residence time of freshwater in OTM with respect to rainfall is on the order of a week, as deduced from a large rainstorm in 1979 (Hamner et al., 1982). The mean residence time of the brackish surface water of Spooky lake, having a tidal amplitude of about half that of lake OTM, is thus expected to be a few weeks. For exact water residence times, which are expected to differ for high and low precipitation periods, a full hydrological study would be required.

Stratification restricts aerobic eukaryotes, such as the usually perennial population of $>10^6$ photosymbiotic jellyfish *Mastigias papua etpisoni*, to the brackish oxygenated surface waters of OTM (Hamner et al., 1982) and supports a thick plate of photosynthetic purple sulfur bacteria, *Chromatium* sp., near the pycno/chemocline of the lakes (Venkateswaran et al., 1993; Fig. 4). Primary productivity is very high in the shallow epilimnion (upper 3 m) of Spooky lake, also giving rise to large amounts of a single species of *Acartia* zooplankton.

The wet climate supports rain forests that contributes plant detritus to the lakes, resulting in highly organic lake bottom sediments (Burnett et al., 1989). On interannual timescales, lake temperatures and salinities are highly sensitive to hydrological variability, so much so that changes in mean lake temperature may precede ENSO variability in the eastern Pacific by three months (Martin et al., 2006). During El Niño events (SOI $<$ 0), decreased precipitation results in an increase in lake surface water salinity and a weakened stratification, and conversely during La Niña events (SOI $>$ 0) increased precipitation causes lower surface salinity and stronger stratification. A rapid transition from strong El Niño to La Niña conditions in 1998–1999 coincided with extreme stratification of OTM and disappearance of all the *Mastigias* medusae, and their photo-endosymbiotic dinoflagellates *Symbiodinium* (Muscatine et al., 1986), for *ca* 1 year.

3. Methods

3.1. Field sampling

A 1085 cm sediment core (SP2-PC) was obtained from Spooky lake in sequential 100 cm sections using a Livingstone-type rod-operated piston corer (Geocore, Columbus, Ohio). Each section was sealed in the field and kept refrigerated at 4 °C until core splitting, imaging and sub-sampling. At 1085 cm sediment depth, carbonate bedrock was reached. In addition, the piston corer was adapted to fit a transparent 10 cm diameter PVC tube and a custom-made rubber piston that allowed intact recovery of a 63 cm long sediment–water interface core (SP3-MW1). A similar 58 cm sediment–water interface core was recovered in lake OTM by SCUBA from a flat area just below the chemocline at 15 m water depth. The euxinic bottom water prohibited coring by SCUBA at the depocenter of the lake. Surface sediment cores were sub-sampled on site in 1 cm intervals and frozen the same day.

Depth profiles of temperature, salinity, dissolved oxygen and oxygen reduction potential were measured using a Hydrolab Quanta meter in both lakes at the time of coring in June, 2004. Spooky, OTM and Clear lake waters were sampled every 1–2 m

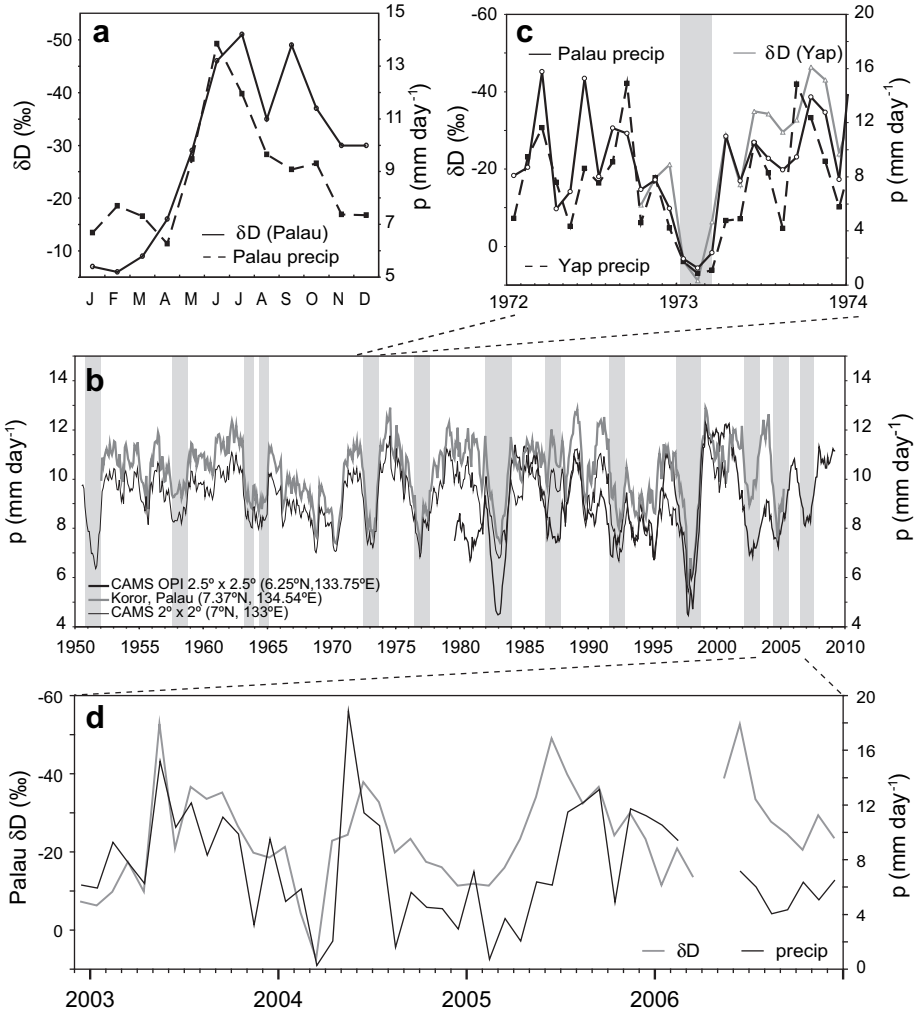

Fig. 3. Relationship between precipitation and its hydrogen isotopic composition (δD_{precip}). (a) Climatological δD_{precip} (Bowen, 2008; available via www.waterisotopes.org) and precipitation (mm day^{-1}) in Palau (Xie and Arkin, 1997). (b). Local and regional precipitation near Palau since 1950. El Niño periods are shaded. Data are rain gauge/satellite data obtained from http://www.ncdc.noaa.gov. (c) Time series of precipitation in Yap and Palau and δD_{precip} in Yap during the 1973 El Niño event. (d) Time series of precipitation and δD_{precip} in Palau during 2003–2006 (Kurita and Ichiyanagi, 2008).

using a Niskin bottle through the entire water column to generate lake water δD depth profiles. Additional samples of lake surface water, precipitation and regional ocean water were collected in June, 2004 during fieldwork. Spooky lake was sampled on 6, 21 and 22 June, and OTM and Clear lake from 20–22 June. Periodic sampling of OTM lake water, regional seawater and precipitation continued through 2004 and 2005 by the Coral Reef Research Foundation in Koror. All samples were sealed, refrigerated and then shipped to the laboratory for later δD analysis.

3.2. Organic geochemical analyses

All sediment samples (0.5–2.0 g dry weight) were freeze dried and extracted by pressurized fluid extraction (Dionex ASE-200) using a 9:1 (v/v) mixture of dichloromethane (DCM) and methanol. Dinosterol (4,23,24-trimethylcholestan-22-en-3β-ol) was isolated following the procedure of Smittenberg and Sachs (2007). Briefly, after the initial solvent extraction, a neutral fraction was isolated by solid phase extraction before further purification using an Agilent 1100 series high-performance liquid chromatograph equipped with a fraction collector and a quadrupole mass spectrometer (HPLC-MS). Dinosterol was separated from co-eluting higher plant-derived pentacyclic triterpenoid alcohols using a DCM-hexane mixture (15:85 v/v, 1 mL/min) on a Prevail Cyano column (4.6 × 250 mm × 5μ). Fractions containing dinosterol were recombined based on HPLC-MS results and then quantified using gas chromatography with flame-ionization detection (GC-FID). Finally, fractions containing dinosterol were acetylated by adding 20 μl pyridine and 20 μl acetic anhydride of known hydrogen isotopic composition and heating at 60 °C for 1 h.

To isolate palmitic acid (PA), fatty acid fractions were initially purified from the total lipid extract using silicious column chromatography (hexane:ethyl acetate:acetic acid; 74:24:2, v/v/v, after previous elution with less polar solvents). The fatty acid fraction was methylated using a mixture of anhydrous methanol and acetyl chloride (9:1 v/v) of known isotopic composition, and further separated in a second chromatography step into fatty acid methyl esters (hexane:ethyl acetate; 95:5, v/v) and hydroxy fatty acids (hexane:ethyl acetate 8:2, v/v).

The stable hydrogen isotopic composition of dinosterol (δD_{Dino}) and palmitic acid (δD_{PA}) were measured on a DELTA V gas chromatograph-isotope ratio mass spectrometer (GC-IRMS) similar to that described by Burgoyne and Hayes (1998). Instrument performance and the H^{3+} factor were determined on a daily basis using

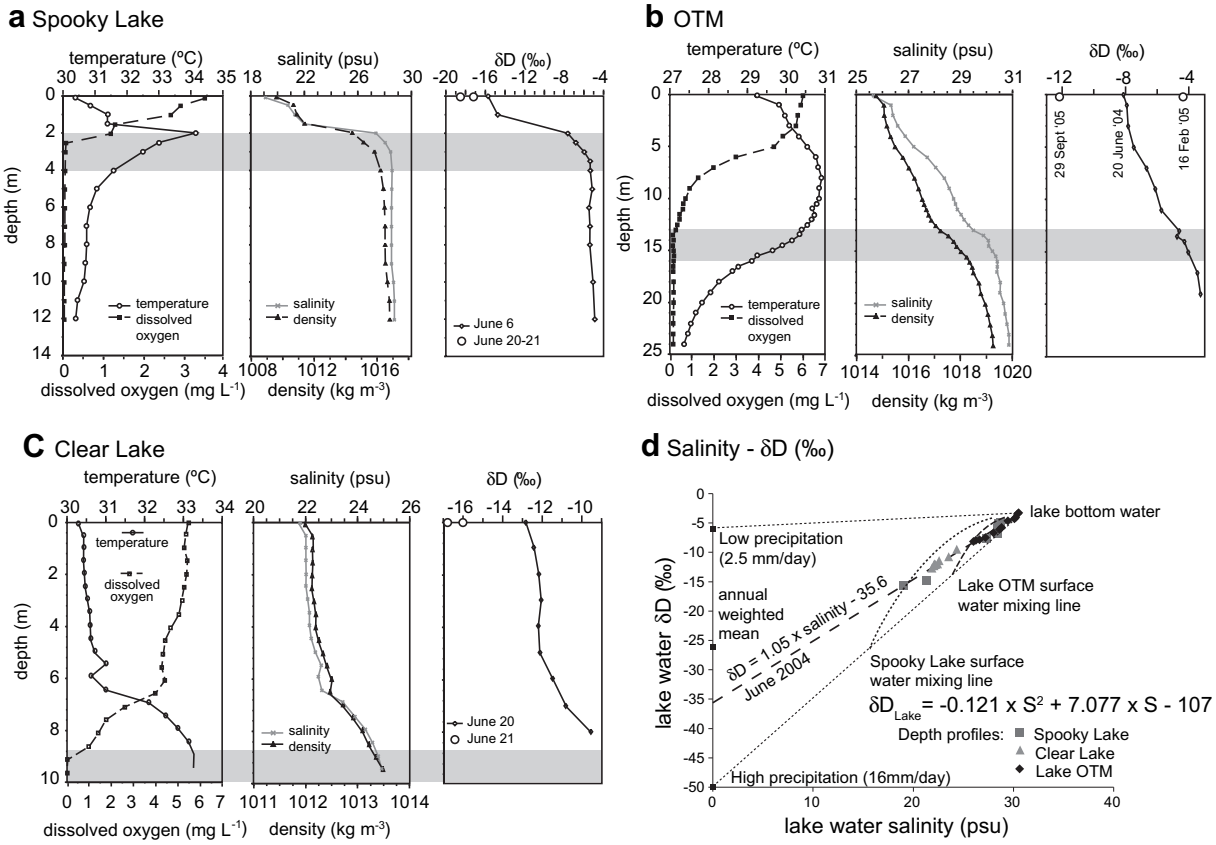

Fig. 4. Depth profiles of Spooky lake, lake OTM and Clear lake temperature, dissolved oxygen, density, salinity and water δD measured in June, 2004. (a) Spooky lake. (b) lake OTM. (c) Clear lake. Depths where photosynthetic sulfur bacterial plates occurred are shaded. For lake OTM, the highest and lowest water δD values observed between June 2004 and November 2005 are also indicated (d). Cross plot of salinity and δD data of a-c, as well as climatological δD values for precipitation. Surface water mixing lines for Spooky lake and lake OTM were constructed as discussed in the text.

a reference gas and a mixture of *n*-alkanes of known isotopic composition as described in Zhang and Sachs (2007). Isotopic values were calculated with ISODAT software using co-injection standards. δD_{Dino} and δD_{PA} were corrected for the hydrogen atoms of the added acetyl and methyl groups, respectively. Hydrogen isotopic values were typically determined by three replicate analyses, and the results were averaged to obtain a mean value and standard deviation. The precision of δD measurements was 4% based on repeated analyses of a standard containing 15 different *n*-alkanes of known δD. δD of lake and ocean water and precipitation (δD_{Precip}) was measured using an H-device Thermo-Finnigan Delta^{plus} XL mass spectrometer at Dartmouth College, as described by Zhang and Sachs (2007).

3.3. Dating

Chronologies for the upper portion of Spooky lake and lake OTM are based on ^{210}Pb dating (Supporting Information, Fig. S1). Radiocarbon dating of acid-alkali-acid treated leaf remains was used to determine the depth of the early 1960s atmospheric bomb spike, the age of the bottommost portion of SP3-MW1, and ages throughout SP2-PC (Supporting Information, Table S1). Measurements were made at the University of California, Irvine's Keck-Carbon Cycle AMS facility, the Woods Hole Oceanographic Institution's National Ocean Sciences AMS facility, and the Lawrence Livermore AMS. Oxcal (v. 4.1) (Bronk Ramsey, 2009) and the Northern Hemisphere atmospheric calibration curve (Reimer et al., 2009) were used to convert to calendar ages.

4. Results

4.1. Limnology and water δD

Temperature, salinity, resulting density, dissolved oxygen contents, and lake water δD profiles (Supplementary Information, Table S2) are shown in Fig. 4. Increases in density in Spooky lake, Clear lake and OTM from about 1009 to 1017, 1012–1014, and 1015–1020 kg m^{-3} correspond to salinity increases from 19 to 29, 22 to 25 and 26 to 31 psu, respectively (Fig. 4a–c). Dissolved oxygen dropped to zero at the pycnocline in the lakes, leading to reducing sulfidic conditions and thick plates of photosynthetic purple sulfur bacteria. Highest temperatures occurred above the bacterial plates, i.e. the pycno/chemocline, but did not inverse the density structure of the water column.

Depth profiles of δD in all three lakes showed trends toward heavier values with depth that strongly resemble salinity and density profiles (Fig. 4). Surface water δD values near −17, −13 and −8‰ in respectively Spooky lake, Clear lake and lake OTM, increased to bottom water values of respectively −5, −9.5 and −3.5‰ (Supplementary Information, Table S2). Local δD_{Precip} of −27 ± 15‰ in June 2004 (Fig. 5a; Supplementary Information, Table S3) were similar to surface lake water, while δD values of −5.8 to −6.4‰ in the saline lagoons nearest OTM were close to lake bottom water δD.

Between June 2004 and September 2005 the δD variability in OTM lake surface water, local precipitation and regional open ocean water show similar seasonal phasing, but significantly different

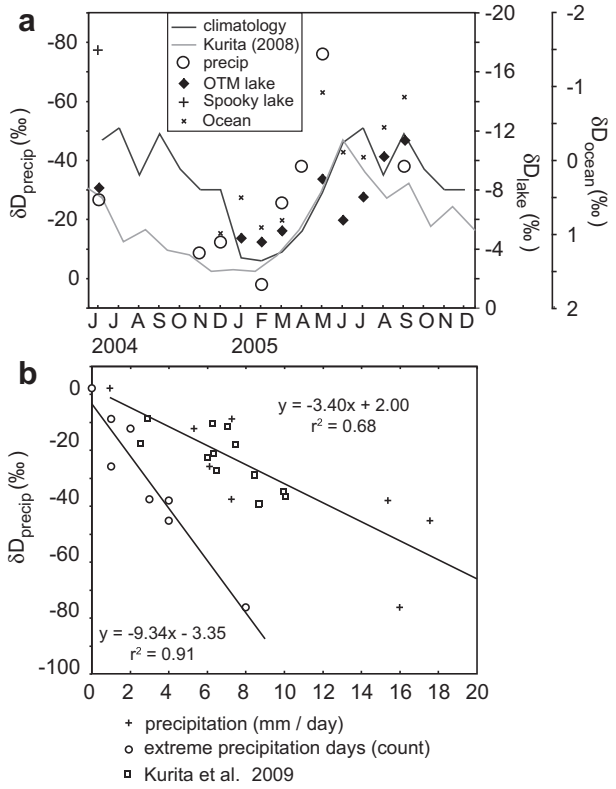

Fig. 5. Seasonal water δD values measured in Palau. (a) Monthly mean δD value of several precipitation samples (open circles), OTM lake surface water (diamonds), Spooky lake surface water (cross) and local ocean water (exes), climatological δD values for Palau, as in Fig. 3 (line). (b) Regression of monthly mean δD_{precip} in Palau with precipitation (crosses) and days of extreme precipitation (open circles). Open squares: long-term (2003–2006) monthly mean δD vs. precipitation amount from Kurita and Ichiyanagi (2008).

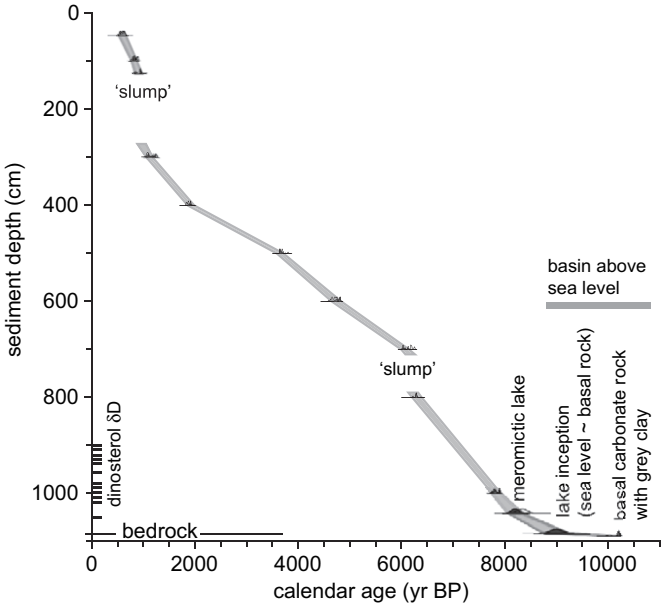

Fig. 6. Age model of the SP2-PC sediment core. Calibrated calendar age probability (2σ) distributions (Table S1) are light shaded and the modeled probability distributions (2σ) are dark shaded. The calibrated points are interpolated with a line with a width of 2σ. The time period for which the basin was above sea level is indicated, as are the approximate timing of lake inception and the estimated time when the lake became meromictic. Bars on the vertical axis indicate depths at which δD_{Dino} was measured.

amplitudes (Fig. 5a, Supplementary Information, Table S3). Lake, precipitation and ocean δD all reach their most enriched values in boreal winter (November–March) and are most depleted in summer (May–September). The amplitude of this variability is largest in precipitation, (2 to −76‰), smaller in OTM lake water (−4.5 to −11.3‰) and smallest in the open ocean (~1 to −1‰).

4.2. Age model

Sediment accumulation rates for OTM-MW1 and SP3-MW1 were determined by fitting exponential decay profiles to plots of accumulated dry mass and excess ^{210}Pb, aided by some radiocarbon measurements (Sachs et al., 2009; Supplementary Information, Fig. S1). The very good fit of the ^{210}Pb data, combined with ^{14}C dates for Spooky lake, results in a well constrained age model for the last century. Uncertainty increases for sediments prior to 1900 AD, when the detection limit of ^{210}Pb is reached but remains constrained by the radiocarbon date at 63 cm depth at the bottom of SP3-MW1. Core SP2-PC was dated using 10 radiocarbon ages (Supplementary Information, Table S1). Based on these radiocarbon ages, combined with information about early Holocene sea-level rise and some stratigraphic information, an age model for this core was constructed (Fig. 6) using the software program Oxcal (v. 4.1; Bronk Ramsey, 2009; Reimer et al., 2009) (see Supplementary Information). Total organic carbon in a 5 cm thick clay layer immediately overlying the carbonate base of SP2-PC was dated 10,230–9940 cal. BP (2σ), an age that likely reflects a mix of older and younger material deposited over several centuries or more prior to inundation of the dry valley (*ca* 24 m below present-day sea level) by post-glacial sea-level rise. Published sea-level curves indicate a rise around Palau as fast as 10–15 mm yr^{-1} until 7 kyr BP (Kayanne et al., 2002), and first inundation of Spooky lake must have happened between 9.3 and 8.7 kyr BP. The shallowest modern lakes that are meromictic (i.e. stratified) are *ca* 5 m–8 m deep. Given this and the rate of sea-level rise, the transition from a holomictic (i.e. mixed, oxic) to a meromictic state where anoxic conditions allow the organic sediment to be better preserved, must have happened between 8.7 and 8.2 kyr BP. Core material from above 1040 cm became less 'peat-like' and also started to include bivalve shell debris. We interpreted this as the boundary between sediments deposited before and after the transition of the lake to a meromictic state. This is indeed expected to be marked by a change in the ecological community structure, including establishment of a numerically large population of the bivalve *Brachidontes* sp., which are especially abundant in all meromictic marine lakes (own observations; G. Paulay, pers. comm.). Between 100 and 200 cm depth the sediment existed almost exclusively of bivalve shell debris, and since these organisms can only grow in oxygenated surface water, we interpreted this as a slump from the side of the lake. Broken shell debris mixed through the otherwise highly organic sediment in the other core sections likely reflects some extent of secondary deposition. The fact that the radiocarbon ages of 600 and 700 cm depth were fairly close to each other (Fig. 6) indicates that this depth interval also contains some mass deposit. However, the otherwise relative straight age model and the absence of reversals in our radiocarbon chronology indicate that the sedimentary succession is generally intact and regular, which is also supported by the very regular ^{210}Pb decay profile of the surface sediment (Supplementary Information, Fig. S1).

4.3. Dinosterol and palmitic acid δD

δD_{PA} values in lake OTM ranged from −165 to −200‰ from 1895 to 1998 A.D. (Fig. 7a; Supplementary Information, Table S4). Spooky

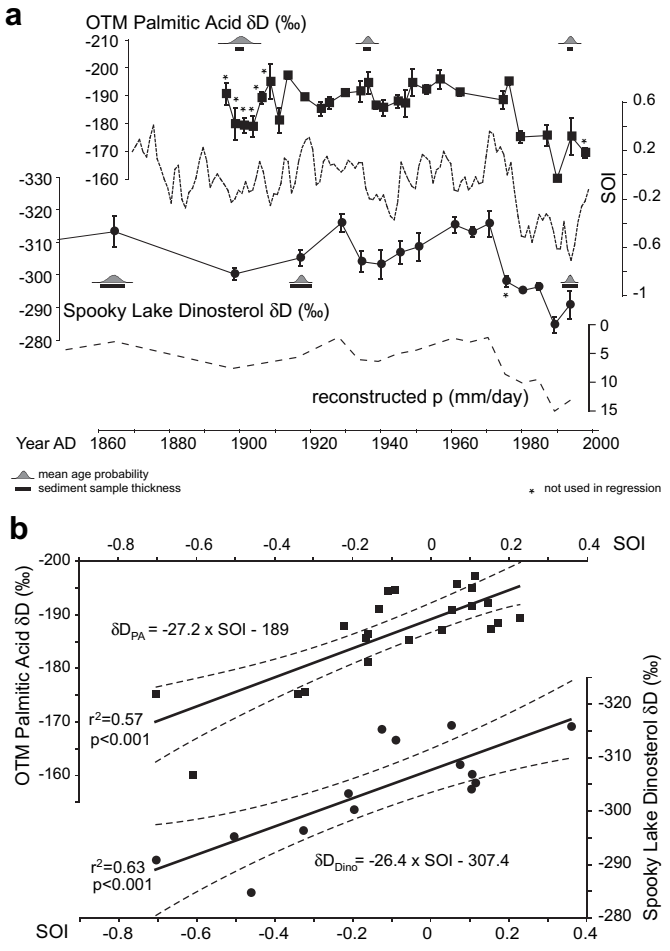

Fig. 7. Relation between lake lipid δD values and the Southern Oscillation Index (SOI). (a) δD_{Dino} (circles) and δD_{PA} (squares) variability since 1870 AD, the instrumental SOI index (9-year running mean) (stippled line). The reconstructed precipitation based on Spooky lake δD_{Dino} is also shown. The time span of the 1-cm thick sediment samples and the probability distribution of the mean sample age of the samples are indicated. b) Linear regressions between the SOI (9-year averages) and δD_{Dino} and δD_{PA}. Dashed lines are 95% confidence intervals. SOI data from University of East Anglia, http://www.cru.uea.ac.uk/cru/data/soi.htm.

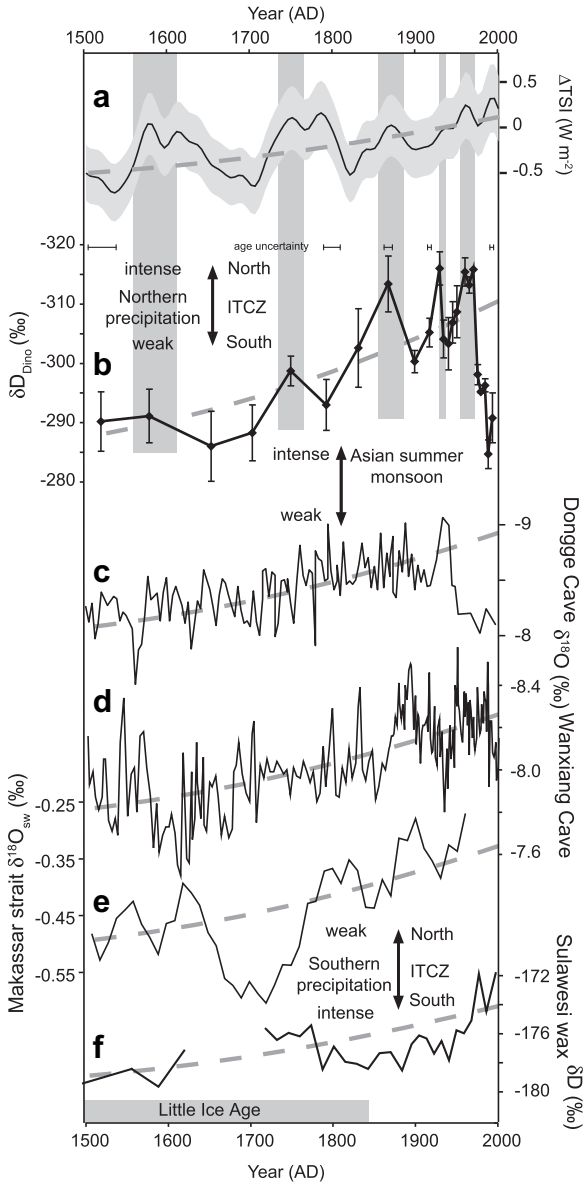

Fig. 8. WPWP hydrologic climate variability since 1500 A.D. (a) 40-year (cycle) averaged total solar irradiance (TSI) anomaly relative to 1986 (1365.57 W m^{-2}) (Steinhilber et al., 2009). Shaded band is 1σ uncertainty. (b) Palau δD_{Dino}. Horizontal error bars indicate the age uncertainty of the record. (c) Dongge Cave speleothem $\delta^{18}O$ (Wang et al., 2005) and (d) Wanxiang Cave speleothem $\delta^{18}O$ (Zhang et al., 2008) indicate Asian summer Monsoon strength. (e) Reconstructed Makassar Strait seawater $\delta^{18}O$ (Oppo et al., 2009). (f) Terrestrial plant-wax δD from Sulawesi deposited in Makassar strait (Tierney et al., 2009). The same polynomial trendline (adjusted for values) is superimposed on all records as a visual aid. Gray bars under records a and b indicate decadal-scale high solar irradiance anomalies corresponding to a relatively wet WPWP. Note the reversed scales for plots e and f.

lake δD_{Dino} values covaried with δD_{PA} during their period of overlap (Fig. 7a), but were offset toward more negative values. Both δD records exhibit an amplitude of ~35‰ during the last century, and highest values occurred after ~1975 A.D. From 1520 – present, δD_{Dino} values from core SP3-MW1 were between −285 and −320‰ (Sachs et al., 2009) (Fig. 8b). Early Holocene (7.0–8.2 kyr BP) δD_{Dino} values from core SP2-PC ranged between −306‰ and −270‰ (Fig. 9a). At the investigated time scale diagenetic alteration of the original, alkyl-carbon bound, isotopic signal is very unlikely (Sessions et al., 2004).

5. Discussion

5.1. Sources of lake water δD variability

Local measurements of δD in precipitation from 2004–2005 indicate that changes in δD_{Precip} are mainly caused by the amount effect. The intensity of precipitation during this interval, estimated by calculating the number of days in each month when precipitation exceeded the long-term mean by at least 1 standard deviation, was highly correlated ($r^2 = 0.91$) with δD_{Precip} (Fig. 5b). δD_{Precip} was moderately correlated ($r^2 = 0.68$) with monthly mean precipitation over this time interval. A similar correlation ($r^2 = 0.70$) between 4 year mean monthly precipitation amount and δD_{Precip} in Palau and Bali was found by Kurita et al. (2009) (Fig. 5b). Their detailed analysis of isotopic ratios in WPWP precipitation indicates that δD_{Precip} is primarily a function of regional precipitation amounts. Precipitation amount, in turn, is ultimately determined by larger scale climate variables like the annual movement of the ITCZ and the intensity of the Walker and Hadley circulations. The intensity of deep convection is also very sensitive to changes in WPWP SST, and small anomalies (~0.5 °C) may generate significant changes in

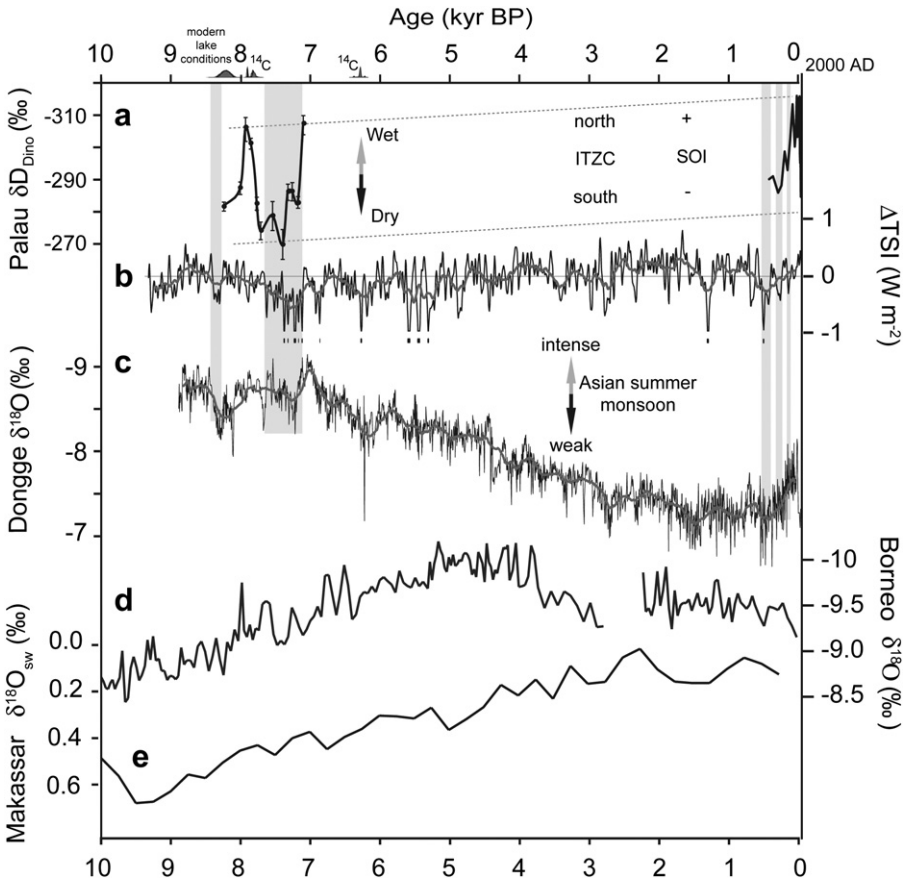

Fig. 9. Comparison of Holocene hydrologic reconstructions. (a) Palau δD_{Dino}. (b) TSI as in Fig. 8, small dots at the bottom indicate TSI < 1364.64 W m^{-2}. (c) Dongge Cave speleothem $\delta^{18}O$ (Wang et al., 2005). Gray bands indicate the concurrence of low TSI, weak precipitation in Palau, and relatively weak Asian summer Monsoon. (d) Difference between August and January insolation at 7°N (Laskar et al., 2004). Compared to the late Holocene, NH seasonality was stronger during the early Holocene due to stronger summer and weaker winter insolation. (e) Borneo speleothem $\delta^{18}O$ (Partin et al., 2007). (f) Reconstructed WPWP mean seawater $\delta^{18}O$ (Stott et al., 2004). (g) Liang Luar stalagmite $\delta^{18}O$ record (Griffiths et al., 2009). Upper horizontal axis: the 2σ age distributions for the calibrated ^{14}C ages of 8 and 10 m are shown (see Fig. 6). The estimated time when lake became meromictic is also indicated.

precipitation amount and intensity (Wang and Mehta, 2008, and references therein).

Assuming that regionally-driven changes in δD_{Precip} are the ultimate source of Palau lake water and seawater δD variability, the *ca* 40‰ change in δD_{Precip} from dry to wet seasons leads to variations of 8‰ in OTM, but only 2‰ in local ocean water (Fig. 5a). This implies that OTM lake water is four times more sensitive than the open ocean with respect to δD_{Precip} variability, and by extension that the lake's δD_{Lipid} record is more sensitive than comparable oceanic proxy records. The more depleted June 2004 Spooky lake water δD (−16‰, Fig. 4a) indicates an even greater dependence of δD_{Lake} on δD_{Precip} in this basin than in OTM, and thus a potentially greater sensitivity of δD_{Lipid} to WPWP hydrologic variability.

The salinities and δD_{water} values measured for the three lakes in June 2004 are well correlated (Fig. 4d), and show a relationship of $\delta D_{water} = 1.05 \times \text{salinity} - 35.6$. This suggests that at the time of sampling precipitation δD averaged approximately −36‰, which is within error of the observed −27 ± 15‰ and similar to mean June–July, 2004 values of −24.1 to −37.6‰ reported by Kurita and Ichiyanagi (2008) for the WPWP. Using lake salinity and δD_{Water} end members (bottom water = 30 psu; δD = −4‰ and precipitation = 0 psu; δD = −36‰) for June 2004 we estimated the fraction of meteoric water in lake surface waters to be *ca* 15% and *ca* 35% for lake OTM and Spooky lake, respectively. This suggests Spooky lake is more than twice as sensitive as lake OTM to precipitation changes, as expected from its much shallower pycnocline.

Making the assumption that the extent of freshwater – seawater mixing of the lakes linearly correlates with the amount of precipitation, and assuming also that δD_{Precip} relates linearly with the amount of rain (Fig. 5b), one can estimate that at the wettest periods (~14 mm/day, with δD_{Precip} as low as −50‰, Figs. 3a and 5a; Kurita et al., 2009), Spooky lake surface water salinity should be ~16 psu, and δD_{Lake} should be ~ −26‰. In contrast, during relatively dry periods surface water δD may become as high as −4‰, and have a salinity of 28 psu, when oceanic and meteoric water have almost the same isotopic composition (Fig. 4d). Calculation for various amounts of rain, their estimated isotopic composition, and the resulting extent of mixing in the different lakes leads to δD-salinity mixing lines, for surface waters, that can be expressed as quadratic equations (Fig. 4d). In other words, lake water δD values respond increasingly sensitive at higher amounts of precipitation, because of the amplifying amount effect. Conversely, the response of δD_{Lake} is smaller at dryer conditions.

5.2. Biomarker δD variability

Laboratory (Englebrecht and Sachs, 2005; Schouten et al., 2006; Zhang and Sachs, 2007; Zhang et al., 2009b) and field (Englebrecht and Sachs, 2005; Huang et al., 2004; Sachse and Sachs, 2008; Schwab and Sachs, 2009) studies demonstrate that δD in a wide range of algal lipids closely co-varies with source water δD. Measurements of salinity, δD_{water} and δD values of

dinoflagellate-produced dinosterol (Volkman, 2003) (δD_{dino}) across large gradients in the Chesapeake Bay (Sachs and Schwab, 2011), confirm that this is also true for this lipid, and that an approximate basal fractionation factor $\epsilon_{dino/water} = -315‰$ applies at zero salinity. Previous work has shown that δD_{PA} in lake surface sediments is capable of recording lake water δD variability (Huang et al., 2004). However, palmitic acid is a generic lipid, which is not only produced by algae (e.g. dinoflagellates) and bacteria (e.g. purple sulfur bacteria), but also by vascular plants. Hence, δD_{PA} may not reflect lake surface water δD exclusively, but may rather represent an integrated ecosystem signal that is ultimately dependent on the δD value of regional precipitation. The advantage of using dinosterol is that it is a specifically algal lipid, in contrast to the generic palmitic acid, which is why we chose dinosterol as a target for Spooky lake. However, purification and isotope analysis of dinosterol is relatively elaborate compared to the more straightforward procedure for palmitic acid. Because of this, and the fact that dinosterol concentrations were relatively low in lake OTM, we chose palmitic acid as a target for this lake. Although they would provide an interesting comparison, laboratory and machine time constraints precluded a parallel δD_{PA} record for Spooky lake.

The generally observed co-variance of δD_{lipid} and source water δD can be modulated by a number of biological and physical factors that influence the extent of fractionation during lipid biosynthesis. For instance, the low δD values of the isoprenoid lipid dinosterol, compared to the higher values of the acetogenic lipid palmitic acid, is caused by the larger extent of D/H fractionation that occurs during isoprenoid lipid synthesis compared to that of acetogenic lipids (Zhang et al., 2009a, 2009b and references therein). Through their impact on biosynthesis and/or metabolism, changes in nutrients, light intensity, salinity and temperature may also influence lipid δD (Sachse and Sachs, 2008; Schouten et al., 2006; Zhang et al., 2009b), leading to variability that is unrelated to changes in source water (c.f. van der Meer et al., 2008). Furthermore, different strains of bacteria, algae and plants have been shown to fractionate D from H differently (Campbell et al., 2009; Sachse et al., 2006; Sauer et al., 2001; Zhang and Sachs, 2007) indicating that changes in biological source could significantly impact the hydrogen isotopic composition of sedimentary lipids. Different species of dinoflagellates may thus, in theory, exert a different D/H fractionation upon dinosterol production. However, in Chesapeake Bay (Sachs and Schwab, 2011), exhibits the same large salinity gradient, (summer) stratification and sub/anoxia as the Palauan lakes, no δD variability could be attributed to changes in species distribution. This apparent absence of a 'species effect' lets us assume that the dinoflagellates in the Palauan lakes, most commonly *Symbiodinium* and *Ceratium* spp., fractionate to a similar extent as those in Chesapeake Bay, although we recognize that the two environments are significantly different, and that we cannot rule out a species effects.

Any influence of temperature on D/H fractionation (Zhang et al., 2009b) is probably small considering that mean lake temperatures have only varied by a few degrees (Dawson et al., 2001). In contrast, recent work shows that the effect of salinity on biosynthetic fractionation appears to be significant. Sachs and Schwab (2011) found a $0.99 \pm 0.23‰$ decrease in D/H fractionation per unit increase in salinity for dinosterol in particulate organic matter along a salinity gradient in Chesapeake Bay. This effect is comparable to that observed by Sachse and Sachs (2008) for various algal lipids analyzed from hypersaline ponds of Christmas Island. The salinity effect amplifies the primary signal of lake water δD variation, so that three additive effects on the recorded δD_{lipid} are at play: (i) Reduced precipitation carries a smaller amount effect; (ii) the lake surface water will experience a relatively greater contribution of δD-enriched oceanic water compared to depleted precipitation, due

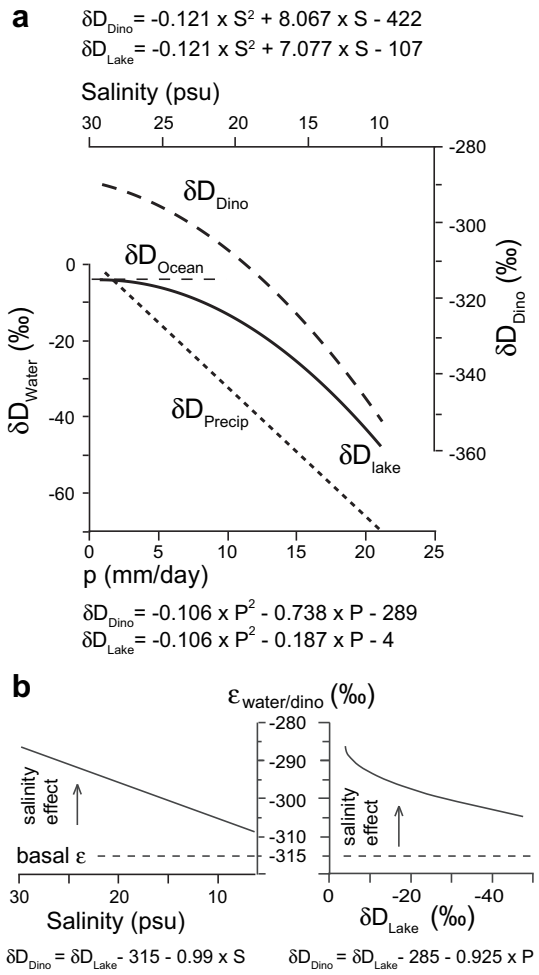

Fig. 10. (a) Relationships between δD values of precipitation, lake water, dinosterol, precipitation amount (p), and salinity (S) in Spooky lake. Equations are based on the relation between p and δD_{Precip}, given in Fig. 5, and the linear relation between S and p in Spooky lake, based on observations (Fig. 4). (b) Dinosterol-water fractionation factor plotted against salinity and δD_{Lake}.

to less mixing; (iii) higher salinities cause diminished D/H fractionation of approximately 1‰/psu. Effects i and ii are discussed above in section 5.2, and can be regarded as a 'source water' effect, while effect iii can be considered a salinity effect. Using the relation between precipitation amount, δD_{precip}, salinity and δD_{Lake} as described in section 5.1 for Spooky lake (Fig. 4d), as well as the salinity effect that decreases the basal fractionation effect of dinosterol ($\epsilon_{water/dino} = -315‰$), one arrives at the relationships given in Fig. 10. Because of the quadratic dependency of δD_{lake} on precipitation and salinity, $\epsilon_{water/dino}$ does not change linearly with δD_{lake}, even though it does with salinity (Fig. 10b). At dry conditions, with high δD_{Lake} and high salinities, $\epsilon_{dino/water}$ changes more per δD_{Lake} unit than at wet conditions. In other words, at wetter conditions the relative influence of the salinity effect (iii) on final δD_{Dino} values becomes less important compared to the source water effect (i + ii), and vice versa.

Between the endmember conditions of Spooky lake (dry: $\delta D_{Lake} = -4‰$; salinity = 28 psu; and wet: $\delta D_{lake} = -26‰$; salinity = 16 psu), δD_{Dino} would differ by 35‰, with salinity accounting for approximately one third of the effect. This is consistent with the range of values that we observe in our record. With the here calculated relationships between precipitation amount, salinity, δD_{Lake}, and δD_{Dino}, it is possible to reconstruct δD_{lake}, precipitation

and salinity of Spooky lake based upon sedimentary δD_{Dino} values (Fig. 7a). We did not calculate the error of the estimates for the derived equations, but it is clear that reconstructed annual average precipitations of near 0 mm/day are unrealistic. This can be explained in part by the insensitivity of δD_{Lake} values toward precipitation at the low end of the precipitation range, primarily caused by the small difference between oceanic and meteoric δD values (Fig. 4d). Furthermore, we did not take the residence time of the lake water into account, which would attenuate the climatic signal. The residence time of the lake water would be expected to be lowest during wet periods, i.e, δD_{Lake} should respond faster to increases in precipitation, than to decreases. The derived equations are not universal, but depend on the local hydrological and meteorological conditions that determine the amount effect and the extent of mixing of rain water into the lake.

The spread of δD_{PA} in lake OTM is similar to that of δD_{Dino} in Spooky lake, even though lake OTM appears more than twice less sensitive from a hydrological perspective. It is possible that part of the PA is not derived from the 'diluted' lake water, but rather from the surrounding vegetation that might transmit the full range of δD_{precip} variability. However, δD values of plant-wax-derived long chain *n*-alkanes in these lakes (unpublished results) show variations that are negligibly larger than the measurement error. Lake OTM δD_{Lake} variability may also be larger than could be deduced from the June 2004 salinity and δD profile. A significant difference with the salinity–δD_{Lake}–δD_{Dino} relationships presented in Sachs and Schwab (2011) for the Chesapeake Bay, is the amplifying role of the amount effect. As exemplified by the difference between lake OTM and Spooky lake (Fig. 4d), the extent of mixing of precipitation into saline waters is also important, as this will affect the salinity-δD_{Water} relationship.

The fact that we can satisfactorily explain the spread of observed δD_{Dino}, based on source water variability and the salinity effect, suggests that these are the two main factors that influence the sedimentary δD_{Dino}, and potentially also δD_{PA}. Although changes in source organisms, nutrients or other biological and physicochemical factors, besides salinity, could also affect δD_{Lipid}, we conclude that these factors appear to be of secondary importance. For example, despite their distinctly different biological sources and biosynthetic pathways, δD_{Dino} and δD_{PA} exhibit synchronous variability that traces regional hydrology, as further described below. This is consistent with the marine lakes being relatively stable ecosystems (Hamner and Hamner, 1998). If any biological response to occasional dramatic climate events influenced δD_{Lipid} independently of the source water and salinity signals, this influence was apparently either relatively unimportant or acted in the same direction as the factors described above.

5.3. Hydrological variability since 1890 AD

The 35‰ range in δD_{Dino} and δD_{PA} since ~1890 AD points to significant hydrological variations during the twentieth century (Fig. 7a). The most striking of these features is the abrupt shift toward drier conditions in the 1970s, which coincides with an anomalous shift toward a tropical Pacific mean state that resembles 'El Niño-like' conditions (Trenberth and Hoar, 1997; Fig. 3b). The Southern Oscillation Index (SOI), captures this variability (Fig. 7a) and can be compared empirically with lipid δD records to assess their utility as hydrological/climatological proxies.

A linear least-squares regression of lipid δD values against 9-year averages of monthly SOI values, with the center corresponding to the given average sediment age values for which biomarker δD values were measured, shows significant inverse correlations for δD_{Dino} ($r^2 = 0.63$ ($p < 0.001$)) and for δD_{PA} ($r^2 = 0.53$ ($p < 0.001$)) (Fig. 7b) (see Supplementary Information). Slopes near $-27‰\ SOI^{-1}$ for both lipids indicate that a 0.1 unit change in the SOI is roughly equivalent to a 3‰ decrease in Palauan lake lipid δD. The 95% confidence interval of the regression indicates that changes in lipid δD of 10‰ or more would predict significantly different values of 0.3–0.5 SOI units, suggesting that δD variability can distinguish dry conditions ('El Niño-like') from 'neutral' and wet conditions ('La Niña-like') (see Supplementary Information).

5.4. Hydrological variability since the Little Ice Age

The modern lipid δD-SOI empirical relation suggests that enriched δD_{Dino} values during the LIA may reflect a more El Niño-like mean state of the tropical Pacific. However, as argued by Sachs et al. (2009), the low LIA δD_{Dino} values can also be explained by a more southerly mean latitude of the ITCZ (Fig. 8). A number of recent records not considered by Sachs et al. (2009) support this interpretation. Speleothem $\delta^{18}O$ evidence suggests the Asian summer monsoon was weaker during the LIA and became progressively stronger during the past five centuries (Wang et al., 2005; Fig. 8c; Zhang et al., 2008; Fig. 8d), consistent with a northward migration of the ITCZ since the LIA. In the southern hemisphere, a foraminifera-based reconstruction of seawater $\delta^{18}O$ (Oppo et al., 2009; Fig. 8e) from the Makassar Strait (4°S, 118°E), and a plant-wax δD record (Tierney et al., 2009; Fig. 8f) from nearby Sulawesi show similar but opposite trends to those in Palau, with wet conditions during the LIA becoming increasingly arid toward the present. These records are consistent with a LIA precipitation pattern resembling that of present-day boreal winter (Fig. 2c), with an intensified South Pacific Convergence Zone (SPCZ) and Australian monsoon rainfall, and diminished northern hemisphere ITCZ precipitation and Asian monsoon activity. The latitude of the ITCZ is known to be sensitive to the inter-hemispheric temperature gradient with southerly displacements occurring when the northern hemisphere is relatively cool (Chiang and Bitz, 2005; Broccoli et al., 2006; Saenger et al., 2009). The distinct minima of total solar irradiance (TSI) that occurred during the LIA (Fig. 8a) may have cooled the northern hemisphere (Shindell et al., 2003) and provide a possible mechanism for the apparent southward position of the ITCZ. The same argument suggests that the general rise in TSI after ~1700 A.D. may have contributed to the centennial scale trend toward wetter conditions in Palau following the LIA (Sachs et al., 2009).

Although meridional migrations of ITCZ/monsoon precipitation appear to exert the dominant control on centennial variations in Palau hydrology, other processes such as ENSO variability and shorter-scale climatic responses to solar, volcanic (Mann et al., 2005), or greenhouse gas-related forcings (Collins et al., 2010), may be more important on (multi) decadal timescales. Although age model uncertainties and record resolution preclude a rigorous statistical comparison, WPWP hydrology inferred from detrended δD_{Dino} (Fig. 8b), appears to co-vary with solar anomalies since 1500 A.D. (Fig. 8a). This is consistent with recent observations of the solar cycle and the Pacific Climate (van Loon et al., 2007, and references therein), and reinforces the notion that more negative δD values, indicating stronger precipitation, occur during periods of relatively high TSI. According to Meehl et al. (2009, and references therein), several mechanisms may explain a large tropical Pacific hydrologic response to relatively small solar forcing. We refrain however from an elaborate discussion about this matter and do not draw any further conclusions, given the limitations of our record and complexity of the issue.

5.5. Early Holocene hydrological variability

Early Holocene (*ca* 8.2–7.0 kyr BP) δD_{Dino} values are on average ~10‰ higher but of similar amplitude as modern values (Fig. 9a).

Highest late Holocene δD_{Dino} values likely reflect a dry state close to endmember conditions, with δD_{precip}, and hence δD_{Lake}, close to that of the ocean. Yet, some of the early Holocene values are even higher. This indicates that either the lake system, or the average water isotopic composition of the WPWP region was different compared to the late Holocene. Alternatively, the basic D/H fractionation factor for dinosterol ($\epsilon_{dino/water}$) was smaller, but, as argued above in section 5.2, this we consider unlikely. Considering the lake system, between 8 and 7 kyr BP sea levels were 1–2 m lower than today (Kayanne et al. (2002), but since Spooky lake had little sediment at the time, it must have been deeper than present. The exchange of water with the open ocean may have been larger resulting in less stratification. However, under that circumstance it would still not be possible for δD_{Lake} to exceed the endmember value of δD_{ocean}. Alternatively, a more isolated lake with a precipitation surplus would experience lower δD values, and only in the case of significant evaporation would the lake become enriched in deuterium. However, this would require a climate that was drastically different from today's, which is considered unlikely (c.f. Oppo et al., 2007). Calling on generally higher water isotope values in the WPWP to explain our early Holocene data corroborates reconstructed $\delta^{18}O$ proxy records of seawater (Stott et al., 2004; Fig. 9f), while models (Oppo et al., 2007) suggest a reduced import of isotopically light water vapor from the Atlantic to the Pacific during the early to mid Holocene. This may have been exacerbated by enhanced export of water vapor from the WPWP onto the adjacent Asian continent, in line with the stronger Asian summer monsoon (LeGrande and Schmidt, 2009; Wang et al., 2005; Fig. 9c). Model results (Oppo et al., 2007) indicate that the resulting saltier WPWP exhibited *ca* 0.5‰ higher $\delta^{18}O$ values than today, and precipitation $\delta^{18}O$ values that were 0.5‰ higher in boreal winter and up to 1.5‰ in boreal summer. Together, these millennial scale hydrologic and water mass changes may account for much of the observed general 10‰ increase of δD_{Dino}.

The similar amplitudes of the early and late Holocene δD_{Dino} records indicate that WPWP hydrologic variability in the early Holocene was similar to recent centuries. Furthermore, this suggests that similar variations in the movement of ITCZ position occurred, and/or the behavior of ENSO occurred during the early Holocene. Although our data do not have a high enough resolution to make any firm conclusions, it does appear that, similar to recent centuries, Palau δD co-varies with the intensity of the Asian monsoon (Wang et al., 2005; Fig. 9c), and with TSI (Steinhilber et al., 2009; Fig. 9b). During the period from 7.7 to 7.2 kyr BP, for instance, high values of δD_{Dino} are congruent with a grand solar minimum, as well as with relatively low speleothem $\delta^{18}O$ values (Fig. 9), similar to the LIA. Indeed, Wang et al. (2005) related periods of weakened summer monsoons, at least in part, to lower TSI.

6. Conclusions

In the marine lakes of Palau, sedimentary δD values of the algal lipid biomarker dinosterol (δD_{Dino}) and the more generic palmitic acid (δD_{PA}) were found to correlate significantly with the Southern Oscillation Index (SOI), which is closely related to hydrological variability in the West Pacific Warm Pool. This indicates that δD values of biomarkers can successfully be used in an empirical sense to reconstruct past hydrologic changes, at least in the Palauan marine lakes. Based on local measurements of lake water and precipitation, combined with literature data of precipitation, we concluded that both δD_{Lake} and δD_{Dino} can interchangeably be expressed as a quadratic function of either precipitation or lake water salinity. At dry conditions δD_{Lake} and δD_{Dino} are less sensitive to hydrological changes, but become increasingly sensitive toward wetter conditions. The quadratic dependence of lake and lipid δD values on precipitation/salinity is due to the combined influence of precipitation amount, and the amount effect within tropical precipitation. Although the basic response of δD_{Dino} is the same as δD_{Lake}, its value is further magnified due to the effect of salinity on the extent of isotopic fractionation between source water and lipid. Theoretical endmember values of δD_{Dino} matched the range of 35‰ observed for the last centuries, which indicates that source water effects and the salinity effect are the main contributors to δD_{lipid} variability.

Paleohydrologic reconstructions based on δD_{Dino} suggest that Palau's climate experienced less intense rainfall during the LIA but became increasingly wet over the past few centuries. In contrast, other records show that southern parts of the WPWP became increasingly dry. This trend likely reflects a more southerly position of mean monsoon/ITCZ precipitation during the LIA, possibly in response to reduced solar irradiance and a cooler northern Hemisphere. Superimposed multi decadal hydrologic variability also appears to be related to solar irradiance, with weaker irradiance inducing an El Niño - like response in the tropical Pacific ocean-atmosphere system, and stronger irradiance promoting a La Niña-like state.

Early Holocene (8.2–7.0 kyr BP) δD_{Dino} values were on average ~10‰ higher than those of recent centuries, which we interpret as a result of millennial scale hydrologic and water mass changes on a global scale. The similar amplitude of ~35‰ indicates that WPWP hydrologic variability in the early Holocene was similar to recent centuries. The highest δD_{Dino} values, reflecting dry conditions, occur during the grand solar minimum between 7.7 and 7.2 kyr BP, while lower values, reflecting wet conditions, are measured for times of higher total solar irradiance. This general relationship is similar to that of the last five centuries, suggesting the same mechanisms were at play.

Although the records presented here are an important step toward understanding WPWP hydrology, verifying our results will require additional paleohydrologic proxy reconstructions from the region that expand upon the still limited spatial and temporal coverage existing at present. Although further field and laboratory testing is necessary to refine the lipid δD_{Lipid} proxy and associated errors/limitations in it's application, the sensitivity of δD_{Lipid} to the tropical climate observed here speaks to its potential in broadly distributed marine lakes (Dawson et al., 2009) to elucidate the climate history across the Pacific region and elsewhere.

Acknowledgments

Funding was provided to J.P.S. by the US National Science Foundation under grants # NSF-ESH-0639640, EAR-0745982, EAR-0823503, and by the Comer Science and Education Foundation. C.P.S. received funding via an NSF Graduate Student Fellowship. We thank the Republic of Palau and Koror State Government for allowing us to work in the marine lakes, as well as Patrick Colin, Lori Bell, and Laura Martin for their logistical assistance. Carolyn Colonero, Orest Kawka, Brittany Demianew and Zhaohui Zhang provided analytical IRMS assistance, while John MacFarlane assisted with ^{210}Pb analysis. The Keck-Carbon Cycle AMS Facility at UC Irvine and Lawrence Livermore National Laboratories are thanked for providing radiocarbon dating.

Appendix. Supplementary information

Supplementary data related to this article can be found online at doi:10.1016/j.quascirev.2011.01.012.

References

Abram, N.J., McGregor, H.V., Gagan, M.K., Hantoro, W.S., Suwargadi, B.W., 2009. Oscillations in the southern extent of the Indo-Pacific warm pool during the mid-Holocene. Quat. Sci. Rev. 28, 2794–2803.

Adler, R.F., 2003. The version-2 global precipitation climatology project (GPCP) monthly precipitation analysis (1979-present). J. Hydromet 4, 1147–1167.

Araguás-Araguás, L., Froehlich, K., Rozanski, K., 1998. Stable isotope composition of precipitation over southeast Asia. J. Geophys. Res. 103 (D22), 28721–28742.

Bard, E., Frank, M., 2006. Climate change and solar variability: What's new under the sun? Earth Planet. Sci. Lett. 248, 1–14.

Behrenfeld, M.J., O'Malley, R.T., Siegel, D.A., McClain, C.R., Sarmiento, J.L., Feldman, G.C., Milligan, A.J., Falkowski, P.G., Letelier, R.M., Boss, E.S., 2006. Climate-driven trends in contemporary ocean productivity. Nature 444, 752–755.

Bowen, G.J., 2008. Spatial analysis of the intra-annual variation of precipitation isotope ratios and its climatological corollaries. J. Geophys. Res. 113. doi:10.1029/2007JD009295 D05113.

Broccoli, A.J., Dahl, K.A., Stouffer, R.J., 2006. Response of the ITCZ to northern hemisphere cooling. Geophys. Res. Lett. 33. doi:10.1029/2005GL024546 L01702.

Brown, J., Tudhope, A.W., Collins, M., McGrego, H.V., 2008. Mid-Holocene ENSO: Issues in quantitative model-proxy data comparisons. Paleoceanography 23. doi:10.1029/2007PA001512 PA3202.

Bronk Ramsey, C., 2009. Bayesian analysis of radiocarbon dates. Radiocarbon 51, 337–360.

Burgoyne, T.W., Hayes, J.M., 1998. Quantitative production of H_2 by pyrolysis of gas chromatographic effluents. Anal. Chem. 70, 5136–5141.

Burnett, W.C., Landing, W.M., Lyons, W.B., Orem, W., 1989. Jellyfish Lake, Palau: a model anoxic environment for geochemical studies. Eos 73, 777–783.

Campbell, B.J., Li, C., Sessions, A.L., Valentine, D.L., 2009. Hydrogen isotopic fractionation in lipid biosynthesis by H2-consuming Desulfobacterium autotrophicum. Geochim. Cosmochim. Acta 73, 2744–2757.

Cane, M.A., 1998. Climate change: a role for the tropical Pacific. Science 282, 59–61.

Chiang, J.C.H., Bitz, C.M., 2005. Influence of high latitude ice cover on the marine Intertropical Convergence Zone. Clim. Dyn. 25, 477–496.

Collins, M., An, S.-I., Cai, W., Ganachaud, A., Guilyardi, E., Jin, F.-F., Jochum, M., Lengaigne, M., Power, S., Timmermann, A., Vecchi, G., Wittenberg, A., 2010. The impact of global warming on the tropical Pacific Ocean and El Niño. Nat. Geosci. 3, 391–397.

Dawson, M.N., Martin, L.E., Bell, L.J., Patric, S., 2009. Marine Lakes. In: Gillespie, R., Clague, D.A. (Eds.), Encyclopedia of Islands. University of California Press, Berkeley, pp. 603–607.

Dawson, M.N., Martin, L.E., Penland, L.K., 2001. Jellyfish swarms, tourists, and the Christ-child. Hydrobiologia 451, 131–144.

Dissard, D., Nehrkea, G., Reichart, G.-J., Bijma, J., 2010. The impact of salinity on the Mg/Ca and Sr/Ca ratio in the benthic foraminifera ammonia tepida: results from culture experiments. Geochim. Cosmochim. Acta 74, 928–940.

Englebrecht, A.C., Sachs, J.P., 2005. Determination of sediment provenance at drift sites using hydrogen isotopes and unsaturation ratios in alkenones. Geochim. Cosmochim. Acta 69, 4253–4265.

Gagan, M.K., Hendy, E.J., Haberle, S.G., Hantoro, W.S., 2004. Post-glacial evolution of the Indo-Pacific Warm Pool and El Niño-southern oscillation. Quat. Int. 118-119, 127–143.

Griffiths, M.L., Drysdale, R.N., Gagan, M.K., Zhao, J., Ayliffe, L.K., Hellstrom, J.C., Hantoro, W.S., Frisia, S., Feng, Y., Cartwright, I., Pierre, E.S., Fischer, M.J., Suwargadi, B.W., 2009. Increasing Australian-Indonesian monsoon rainfall linked to early Holocene sea-level rise. Nat. Geosci. 2, 636–639.

Hamner, W.M., Gilmer, R.W., Hamner, P.P., 1982. The physical, chemical, and biological characteristics of a stratified, saline, sulfide lake in Palau. Limnol. Oceanogr. 27, 896–909.

Hamner, W.M., Hamner, P.P., 1998. Stratified marine lakes of Palau (Western Caroline Islands). Phys. Geogr. 19, 175–220.

Huang, Y.S., Shuman, B., Wang, Y., Webb, T., 2004. Hydrogen isotope ratios of individual lipids in lake sediments as novel tracers of climatic and environmental change: a surface sediment test. J. Paleolim. 31, 363–375.

IAEA, 2006. Isotope Hydrology Information System. The ISOHIS Database. http://isohis.iaea.org Accessible at.

Kayanne, H., Yamano, H., Randall, R.H., 2002. Holocene sea-level changes and barrier reef formation on an oceanic island, Palau Islands, western Pacific. Sed. Geol. 150, 47–60.

Kurita, N., Ichiyanagi, K., 2008. Daily basis precipitation sampling network for water isotope analysis. Institute of Observational Research for Global Change, Japan Agency for Marine-Earth Science and Technology. http://www.jamstec.go.jp/iorgc/hcorp/data/.

Kurita, N., Ichiyanagi, K., Matsumoto, J., Yamanaka, M.D., Ohata, T., 2009. The relationship between the isotopic content of precipitation and the precipitation amount in tropical regions. J. Geochem. Explor. 102, 113–122.

Laskar, J., Robutel, P., Joutel, F., Gastineau, M., Correia, A.C.M., Levrard, B., 2004. A long term numerical solution for the insolation quantities of the Earth. Astron. Astrophys. 428, 261–285.

LeGrande, A.N., Schmidt, G.A., 2009. Sources of Holocene variability of oxygen isotopes in paleoclimate archives. Clim. Past 5, 441–455.

Legates, D.R., Willmott, C.J., 1990. Mean seasonal and spatial variability in gauge-corrected, global precipitation. Int. J. Climatol. 10, 111–127.

Mann, M.E., Cane, M.A., Zebiak, S.E., Clement, A., 2005. Volcanic and solar forcing of the tropical Pacific over the past 1000 years. J. Clim. 18, 447–456.

Martin, L.E., Dawson, M.N., Bell, L.J., Colin, P.L., 2006. Marine lake ecosystem dynamics illustrate ENSO variation in the tropical western Pacific. Biol. Lett. 2, 144–147.

Meehl, G.A., Arblaster, J.M., Matthes, K., Sassi, F., van Loon, H., 2009. Amplifying the Pacific climate system response to a small 11-year solar cycle forcing. Science 325, 1114.

Muscatine, L., Wilkerson, F.P., McCloskey, L.R., 1986. Regulation of population density of symbiotic algae in a tropical marine jellyfish (Mastigias sp.). Mar. Ecol. Prog. Ser. 32, 279–290.

Newton, A., Thunell, R., Stott, L., 2006. Climate and hydrographic variability in the Indo-Pacific Warm Pool during the last millennium. Geophys. Res. Lett. 33. doi:10.1029/2006GL027234 L19710.

Oppo, D.W., Schmidt, G.A., LeGrande, A.N., 2007. Seawater isotope constraints on tropical hydrology during the Holocene. Geophys. Res. Lett. 34. doi:10.1029/2007GL030017 L13701.

Oppo, D.W., Rosenthal, Y., Linsley, B.K., 2009. 2,000-year-long temperature and hydrology reconstructions from the Indo-Pacific Warm Pool. Nature 460, 1113–1116.

Partin, J.W., Cobb, K.M., Adkins, J.F., Clark, B., Fernandez, D.P., 2007. Millennial-scale trends in west Pacific Warm Pool hydrology since the last glacial maximum. Nature 449, 452–455.

Pierrehumbert, R.T., 2000. Climate change and the tropical Pacific: the sleeping dragon wakes. Proc. Nat. Acad. Sci. 97, 1355–1358.

Reimer, P.J., Baillie, M.G.L., Bard, E., Bayliss, A., Beck, J.W., Blackwell, P.G., Bronk Ramsey, C., Buck, C.E., Burr, G.S., Edwards, R.L., Friedrich, M., Grootes, P.M., Guilderson, T.P., Hajdas, I., Heaton, T.J., Hogg, A.G., Hughen, K.A., Kaiser, K.F., Kromer, B., McCormac, F.G., Manning, S.W., Reimer, R.W., Richards, D.A., Southon, J.R., Talamo, S., Turney, C.S.M., van der Plicht, J., Weyhenmeyer, C.E., 2009. IntCal09 and Marine09 radiocarbon age calibration curves, 0-50,000 years cal BP. Radiocarbon 51, 1111–1150.

Sachs, J.P., Sachse, D., Smittenberg, R.H., Zhang, Z., Battisti, D.S., Golubic, S., 2009. Southward movement of the Pacific intertropical convergence zone AD 1400–1850. Nat. Geosci. 2, 519–525.

Sachs, J.P., Schwab, V.F., 2011. Hydrogen isotopes in dinosterol from the Chesapeake Bay estuary. Geochim. Cosmochim. Acta 75, 444–459.

Sachse, D., Radke, J., Gleixner, G., 2006. delta D values of individual n-alkanes from terrestrial plants along a climatic gradient - Implications for the sedimentary biomarker record. Org. Geochem. 37, 469–483.

Sachse, D., Sachs, J.P., 2008. Inverse relationship between D/H fractionation in cyanobacterial lipids and salinity in Christmas Island saline ponds. Geochim. Cosmochim. Acta 72, 793–806.

Sauer, P.E., Eglinton, T.I., Hayes, J.M., Schimmelmann, A., Sessions, A.L., 2001. Compound-specific D/H ratios of lipid biomarkers from sediments as a proxy for environmental and climatic conditions. Geochim. Cosmochim. Acta 65, 213–222.

Saenger, C., Cohen, A.C., Oppo, D.W., Hubbard, D.H., 2008. Interpreting sea surface temperature from strontium/calcium ratios in Montastrea corals: link with growth rate and implications for proxy reconstructions. Paleoceanography 23. doi:10.1029/2007PA001572.

Saenger, C., Chang, P., Ji, L., Oppo, D.W., Cohen, A.L., 2009. Tropical Atlantic climate response to low-latitude and extratropical sea-surface temperature: a Little Ice Age perspective. Geophys. Res. Lett. 36. doi:10.1029/2009GL038677 L11703.

Schouten, S., Ossebaar, J., Schreiber, K., Kienhuis, M.V.M., Langer, G., Benthien, A., Bijma, J., 2006. The effect of temperature, salinity and growth rate on the stable hydrogen isotopic composition of long chain alkenones produced by *Emiliania Huxleyi* and *Gephyrocapsa Oceanica*. Biogeosciences 3, 113–119.

Schwab, V.F., Sachs, J.P., 2009. The measurement of D/H ratio in alkenones and their isotopic heterogeneity. Org. Geochem. 40, 111–118.

Sessions, A.L., Sylva, S.P., Summons, R.E., Hayes, J.M., 2004. Isotopic exchange of carbon-bound hydrogen over geologic timescales. Geochim. Cosmochim. Acta 68, 1545–1559.

Shindell, D.T., Schmidt, G.A., Miller, R.L., Mann, M.E., 2003. Volcanic and solar forcing of climate change during the preindustrial era. J. Clim. 16, 4094–4107.

Smittenberg, R.H., Sachs, J.P., 2007. Purification of dinosterol for hydrogen isotopic analysis using high-performance liquid chromatography-mass spectrometry. J. Chrom. A. 1169, 70–76.

Spencer, R.W., 1993. Global oceanic precipitation from the MSU during 1979-91 and comparisons to other climatologies. J. Clim. 6, 1301–1326.

Steinhilber, F., Beer, J., Fröhlich, C., 2009. Total solar irradiance during the Holocene. Geophys. Res. Lett. 36. doi:10.1029/2009GL040142 L19704.

Stott, L., Cannariato, K., Thunell, R., Haug, G.H., Koutavas, A., Lund, S., 2004. Decline of surface temperature and salinity in the western tropical Pacific Ocean in the Holocene epoch. Nature 431, 56–59.

Tierney, J.E., Oppo, D.W., Rosenthal, Y., Russell, J.M., Linsley, B.K., 2009. Coordinated hydrological regimes in the Indo-Pacific region during the past two millennia. Paleoceanography. doi:10.1029/2009PA001871.

Trenberth, K.E., Branstator, G.W., Karoly, D., Kumar, A., Lau, N.-C., Ropelewski, C., 1998. Progress during TOGA in understanding and modeling global teleconnections associated with tropical sea surface temperatures. J. Geophys. Res. 103 (C7), 14291–14324.

Trenberth, K.E., Hoar, T.J., 1997. El Niño and climate change. Geophys. Res. Lett. 24, 3057–3060.

van der Meer, M.T.J., Sangiorgi, F., Baas, M., Brinkhuis, H., Sinninghe Damsté, J.S., Schouten, S., 2008. Molecular isotopic and dinoflagellate evidence for Late Holocene freshening of the Black Sea. Earth Planet. Sci. Lett. 267, 426–434.

van Loon, H., Meehl, G.A., Shea, D.J., 2007. Coupled air-sea response to solar forcing in the Pacific region during northern winter. J. Geophys. Res. 112. doi:10.1029/2006JD007378.

Venkateswaran, K., Shimada, A., Maruyama, A., Higashihara, T., Sakou, H., Maruyama, T., 1993. Microbial characteristics of Palau Jellyfish lake. Can. J. Microbiol. 39, 506–512.

Volkman, J., 2003. Sterols in microorganisms. Appl. Microbiol. Biotechnol. 60, 495–506.

Wang, Y., Cheng, H., Edwards, R.L., He, Y., Kong, X., An, Z., Wu, J., Kelly, M.J., Dykoski, C.A., Li, X., 2005. The Holocene Asian monsoon: links to solar changes and North Atlantic climate. Science 308, 854–857.

Wang, H., Mehta, V.M., 2008. Decadal variability of the Indo-Pacific warm pool and its association with atmospheric and oceanic variability in the NCEP–NCAR and SODA reanalyses. J. Clim. 21, 5545–5565.

Woodward, F.I., Lomas, M.R., Quaife, T., 2008. Global responses of terrestrial productivity to contemporary climatic oscillations. Phil. Trans. Roy. Soc. Lond. B. 363, 2779–2785.

Wu, H.C., Grottoli, A.G., 2010. Stable oxygen isotope records of corals and sclerosponge in the Western Pacific warm pool. Coral Reefs 29, 413–418.

Xie, P.P., Arkin, P.A., 1997. Global precipitation: a 17-year monthly analysis based on gauge observations, satellite estimates, and numerical model outputs. Bull. Am. Meteorol. Soc. 78, 2539–2558.

Yancheva, G., Nowaczyk, N.R., Mingram, J., Dulski, P., Schettler, G., Negendank, J.F.W., Liu, J., Sigman, D.M., Peterson, L.C., Haug, G.H., 2007. Influence of the intertropical convergence zone on the East Asian monsoon. Nature 445, 74–77.

Yan, X.-H., Ho, C.-R., Zheng, Q., Klemas, V., 1992. Temperature and size variabilities of the western Pacific warm pool. Science 258, 1643–1645.

Zhang, Z., Sachs, J.P., 2007. Hydrogen isotope fractionation in freshwater algae: I. Variations among lipids and species. Org. Geochem. 38, 582–608.

Zhang, X., Gillespie, A.L., Sessions, A.L., 2009a. Large D/H variations in bacterial lipids reflect central metabolic pathways. Proc. Nat. Acad. Sci. 106, 12580.

Zhang, Z., Sachs, J.P., Marchetti, A., 2009b. Hydrogen isotope fractionation in freshwater and marine algae: II. Temperature and nitrogen limited growth rate effects. Org. Geochem. 40, 428–439.

Zhang, P.Z., Cheng, H., Edwards, R.L., Chen, F., Wang, Y., Yang, X., Liu, J., Tan, M., Wang, X., Liu, J., An, C., Dai, Z., Zhou, J., Zhang, D., Jia, J., Jin, L., Johnson, K.R., 2008. A test of climate, sun, and culture relationships from an 1810-year Chinese cave record. Science 322, 940–942.